Applied Surface Science 302 (2014) 163–168

Contents lists available at ScienceDirect

Applied Surface Science

journal homepage: www.elsevier.com/locate/apsusc

A novel patterning effect during high frequency laser micro-cutting of hard ceramics for microelectronics applications

Guillaume Savriama[a,b,*], Vincent Jarry[b], Laurent Barreau[b], Chantal Boulmer-Leborgne[a], Nadjib Semmar[a]

[a] GREMI-UMR 7344, CNRS/Univ-Orléans, 14 rue d'Issoudun, BP 6744, F-45067 Orléans, France
[b] STMicroelectronics, 10 rue Thalès de Milet, CS 97155, 37071 Tours Cedex 2, France

ARTICLE INFO

Article history:
Received 24 June 2013
Received in revised form 13 February 2014
Accepted 15 February 2014
Available online 24 February 2014

Keywords:
Laser micromachining
Sapphire
Glass
Phase explosion
Microelectronics industry

ABSTRACT

This paper investigates the laser micro-cutting of wide band gap materials for microelectronics industry purposes. An ultraviolet (355 nm) diode-pumped solid-state (DPSS) nanosecond laser was used in this investigation. The laser energy varied from 7 to 140 μJ/pulse with typical frequencies from 40 to 200 kHz. The effect of pulse energy and scanning speed on the depth of the cutting street of α-Al_2O_3 and glass was studied. Typical depths of 200 μm were achieved on α-Al_2O_3 for 140 μJ/pulse, 40 kHz at 13 mm/s. SEM images showed periodic patterns produced by periodic explosive boiling that can influence the achieved depth. The shape, size and periodicity of the recast material depended on the feed rate and the laser beam frequency. This periodic removal mechanism seems to be specific to dielectrics since it was not observed for semiconductors such as silicon or silicon carbide.

1. Introduction

For nanosecond lasers, damage usually occurs via conventional heating in transparent dielectrics [1]. The electrons are located in the valence band and are separated from the conduction band by an optical band gap. The photon energy of the present system was 3.5 eV and was not sufficient to promote an electron from the valence to the conduction band. It was shown in Ref. [2] that the α-Al_2O_3 used here contained impurities, defects and inter-band transitions. This is responsible for non-linear absorption of the incident light and initiates the transfer of energy to the matter. In such a case, the ablation mechanism will likely be similar to that of a metal [3–5]. The main issue is that this ablation regime depends on the seed electrons and the laser intensity. The impurities absorb the incident radiation and transfer the heat energy to the lattice by carrier-phonon coupling. The material is then heated until its melting point. The surface of the liquid is then vaporized, and the vapour exerts a recoil pressure which ejects part of the remaining liquid. The phenomenon of phase explosion or explosive boiling has also been reported in the literature [6,7]. This mechanism occurs as the superheated liquid reaches 0.8–0.9 times the thermodynamic critical temperature "T_c" which is around 5335 K for α-Al_2O_3 [8] and 4000 K for CB6 red glass variety [9]. The system is then a mixture of vapour and superheated liquid droplets (nuclei). On reaching a certain density, they are ejected explosively. Phase explosion thus occurs, provided that both thermodynamic (temperature ~ 0.8–0.9 "T_c") and kinetic (sufficient time "τ_c" to allow the nuclei to reach a critical size "*dc*") conditions are met. Refs. [10,11] suggested that a high power density of 10^{10} W/cm^2 is required. However, Han et al. [9], using a lower power density of 10^8 W/cm^2 at 355 nm, indicated that the high repetition frequency has a role to play for glass. Stoian et al. [12] also mentioned the effect of multi-shots on the occurrence of phase explosion for α-Al_2O_3. A previous paper [2] revealed that for high overlap ratios, periodic explosive boiling could occur, leading to an undesirable larger Heat Affected Zone (HAZ). Reducing the cutting width is critical in the microelectronics industry to increase the gross die (number of chips per wafer), as this increases the throughput and reduces the production steps and material consumption. The present study aims at extending our knowledge of the parameters that influence explosive boiling in ceramic substrates.

2. Experimental details

The processing source was a DPSS Nd:YAG laser that is part of an industrial machine built to manage several wafers, and com-

* Corresponding author at: GREMI-UMR 7344, CNRS/Univ-Orléans, 14 rue d'Issoudun, BP 6744, F-45067 Orléans, France. Tel.: +33 247428112.
E-mail addresses: guillaume.savriama@gmail.com, guillaume.savriama@st.com (G. Savriama).

http://dx.doi.org/10.1016/j.apsusc.2014.02.077
0169-4332/

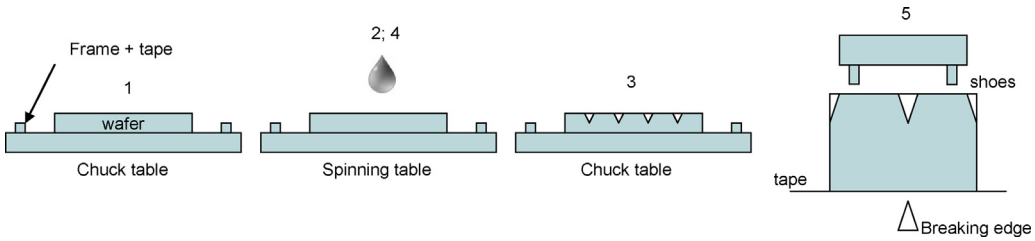

Fig. 1. Schematic view of laser/breaking process. (1) Mount wafer, (2) clean wafer, (3) laser irradiation, (4) clean and (5) focus on breaking step.

prises a cleaning/coating station. The source delivers a laser beam at 355 nm wavelength in the nanosecond regime. 7–140 μJ/pulse can be delivered with typical repetition rates of 40–200 kHz. It is important to note that the pulse duration increases with the frequency from 90 ns at 40 kHz to 300 ns at 200 kHz (for reasons of confidentiality, no further details can be disclosed). The theoretical spot size is 5 μm and the intensity range is between 0.5 and 7.5 GW/cm^2. The laser head is fixed and the chuck table moves along the *X* and *Y* axes at speeds up to 600 mm/s. The process used here is a scribe/break method [13,14]. A thin blade is aligned with the laser groove and two "shoes" at the surface push the wafer down. Fig. 1 shows a schematic view of the process.

The absorption coefficient of sapphire and glass were determined using a UVISEL-VIS ellipsometer for data acquisition and the software Delta Psi 2 from Horiba to model the optical spectra.

Groove width and depth were observed and analyzed using an S-4160 scanning electron microscope (SEM) from Hitachi and a Hisomet microscope from Optica. Industrial 610 μm thick α-Al_2O_3 with an (0 1 2) orientation from CrystalQ was used for this study. X-ray diffraction spectrometry (XRD) was performed in a previous study [2]. Some unidentified peaks and miscuts revealed the presence of contamination or defects. Contrary to what is announced by the manufacturer, the material was found to be polycrystalline ((1 1 3) orientation was identified in addition to the (0 1 2) one).

The glass substrate was the borofloat 33 varieties provided by Schott and was originally 1200 μm thick. It was ground to a thickness of 200 μm. It had a 1.2 μm Undoped Silica Glass (USG) layer on the surface. The glass was tested both with and without the 10–12 μm thick PBO (poly(p-phenylene benzobisoxanole)) layer which is spin coated in the front-end area.

3. Results and discussion

3.1. Sapphire and glass properties

At 355 nm, the absorption coefficient for α-Al_2O_3 was ~1.3×10^4 cm^{-1} which corresponds to a penetration depth of ~770 nm. This shows that linear absorption occurred and that thermal ablation took place. For borofloat, the absorption coefficient was only ~445 cm^{-1} which corresponds to a penetration depth of ~ 22.5 μm. This suggests that borofloat is mainly transparent and that there was insufficient linear absorption to initiate an energy build-up and an ablation process. Those results were obtained by ellipsometry [2,15]. The following experiment was conducted in order to verify the assumption of non-linear absorption phenomenon explained in Section 1.

A scanning speed of 600 mm/s was used to obtain resolved spot and estimate the correct spot size and overlap ratio for each energy value (10 μm approximation in previous work [2]). Instead of obtaining a series of craters separated by 15 μm (centre to centre) from each other, we obtained a few random dots at low energies. Indeed, non-linear absorption is usually enhanced by high intensities [3–5] and also depends on the random distribution of seed electrons in the bulk for nanosecond pulses. The deterministic

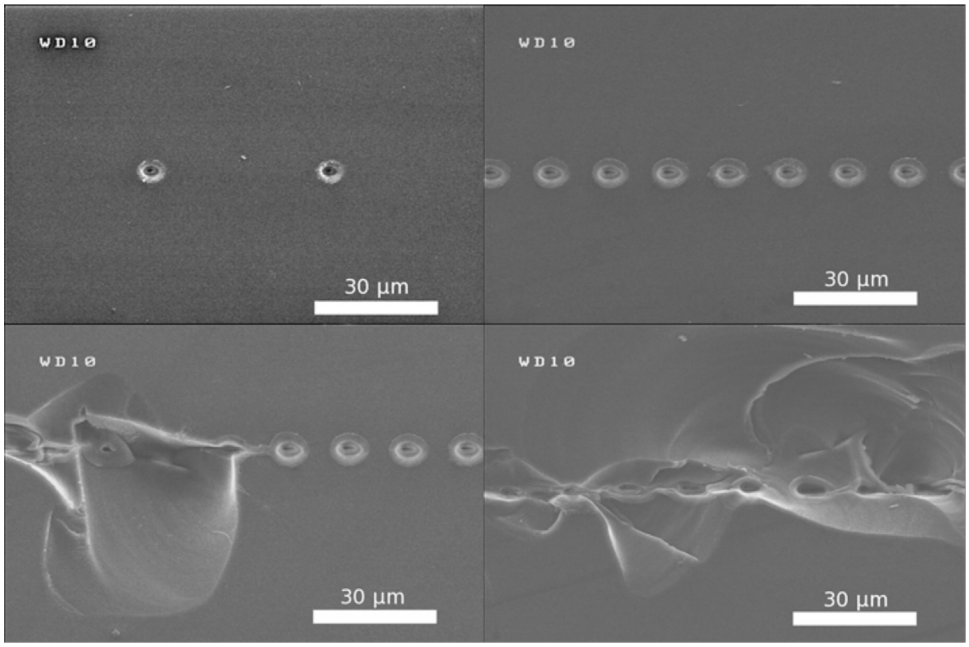

Fig. 2. Illustration of the probabilistic beam absorption related to distribution of impurities in borofloat. The frequency and scanning speed were respectively fixed at 40 kHz and 600 mm/s in order to obtain a resolved pulse. From left to bottom right: 45, 95, 120, 145 μJ/pulse.